Anal Bioanal Chem (2011) 401:3249–3261
DOI 10.1007/s00216-011-5436-y

ORIGINAL PAPER

# Quantitative profiling of tryptophan metabolites in serum, urine, and cell culture supernatants by liquid chromatography–tandem mass spectrometry

**Wentao Zhu · Axel P. Stevens · Katja Dettmer · Eva Gottfried · Sabine Hoves · Marina Kreutz · Ernst Holler · André B. Canelas · Ido Kema · Peter J. Oefner**

Received: 17 August 2011 / Revised: 21 September 2011 / Accepted: 21 September 2011 / Published online: 8 October 2011


**Abstract** A sensitive, selective, and comprehensive method for the quantitative determination of tryptophan and 18 of its key metabolites in serum, urine, and cell culture supernatants was developed. The analytes were separated on a C18 silica column by reversed-phase liquid chromatography and detected by electrospray ionization tandem mass spectrometry in positive ion multiple reaction monitoring (MRM) mode, except for indoxyl sulfate which was measured in negative ion MRM mode in a separate run. The limits of detection and lower limits of quantification were in the range of 0.1–50 and 0.5–100 nM, respectively. Fully $^{13}C$ isotope-labeled and deuterated internal standards were used to achieve accurate quantification. The applicability of the method to analyze serum, urine, and cell culture supernatants was demonstrated by recovery experiments and the evaluation of matrix effects. Precision for the analysis of serum, urine, and cell culture supernatants ranged between 1.3% and 16.0%, 1.5% and 13.5%, and 1.0% and 17.4%, respectively. The method was applied to analyze changes in tryptophan metabolism in cell culture supernatants from IFN-γ-treated monocytes and immature or mature dendritic cells.

**Keywords** Tryptophan metabolism · LC-MS/MS · Serum · Urine · Cell culture supernatant

## Introduction

L-Tryptophan (Trp) is an essential amino acid that is required for the biosynthesis of proteins and functions as a precursor of many biologically active substances. As shown in Fig. 1, Trp catabolism proceeds mainly via three pathways in mammalians [1]: the kynurenine and serotonin

**Electronic supplementary material** The online version of this article (doi:10.1007/s00216-011-5436-y) contains supplementary material, which is available to authorized users.

W. Zhu · A. P. Stevens · K. Dettmer · P. J. Oefner (✉)
Institute of Functional Genomics, University of Regensburg,
Josef-Engert-Str. 9,
93053 Regensburg, Germany
e-mail: peter.oefner@klinik.uni-regensburg.de

E. Gottfried · M. Kreutz · E. Holler
Department of Hematology and Internal Oncology,
University Hospital Regensburg,
Franz-Josef-Strauss-Allee 11,
93053 Regensburg, Germany

S. Hoves
Division of Clinical Pharmacology,
Ludwig-Maximilian University of Munich,
Ziemssenstr. 1,
80336 Munich, Germany

A. B. Canelas
Department of Biotechnology, Kluyver Centre for Genomics
of Industrial Fermentation, Delft University of Technology,
Julianalaan 67,
2628 BC Delft, The Netherlands

I. Kema
Department of Laboratory Medicine, University Medical Center,
University of Groningen,
9700 RB Groningen, The Netherlands

*Present Address:*
A. P. Stevens
Analytical Department,
Helmholtz Centre for Environmental Research UFZ,
Permoserstr. 15,
04318 Leipzig, Germany

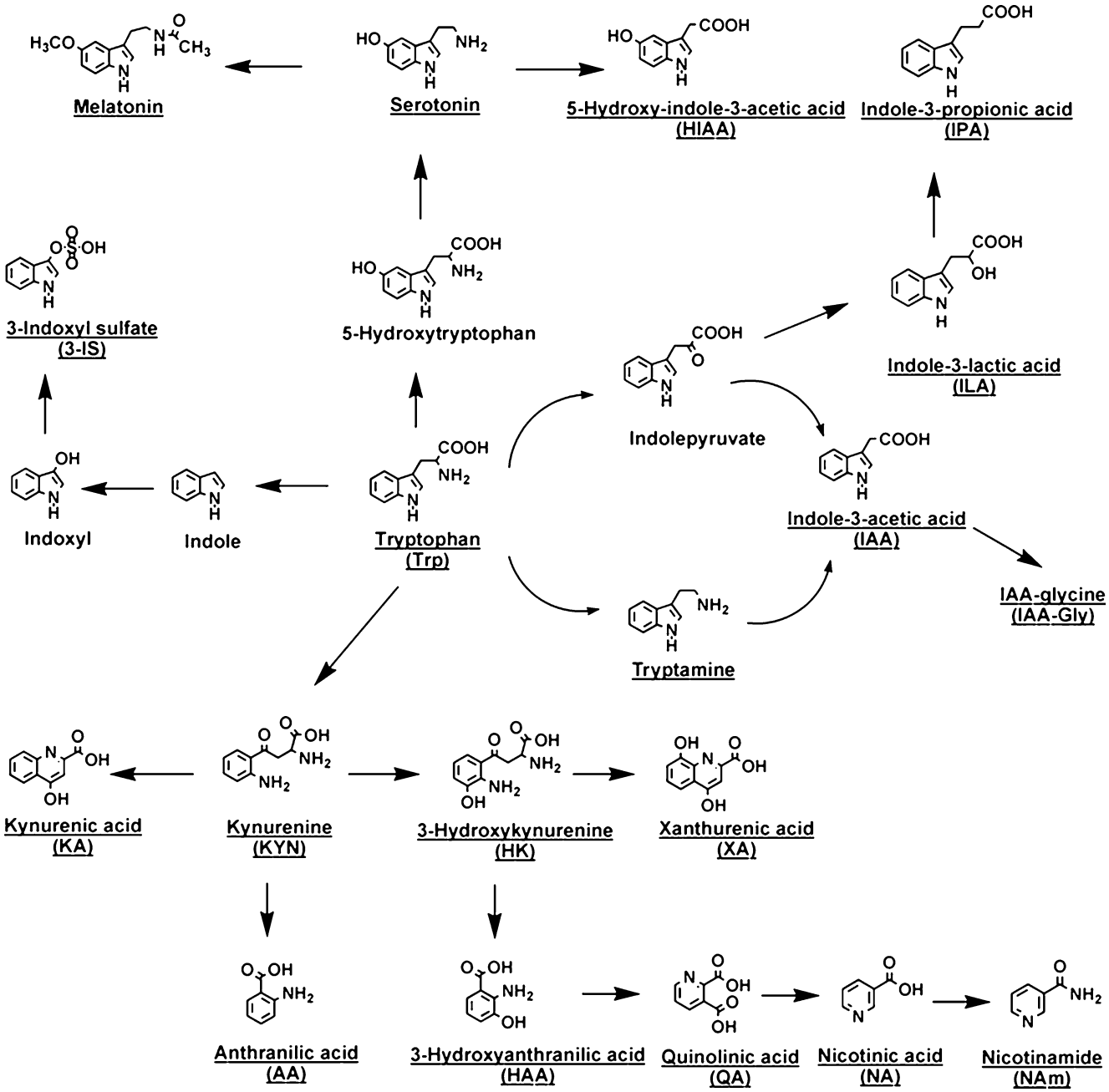


**Fig. 1** Scheme of tryptophan metabolism. *Underlined* metabolites were measured by the LC-MS/MS method described

pathways as well as bacterial degradation. Intestinal bacteria metabolize Trp to indole, which is further metabolized to 3-indoxyl sulfate (3-IS) in the liver. The latter is a uremic toxin that is normally excreted into urine, but has been found to accumulate in serum of patients with chronic kidney disease [2]. A smaller percentage of Trp is converted by bacteria into indole-3-acetic acid (IAA), indole-3-propionic acid (IPA), and indole-3-lactic acid (ILA). Intestinal microorganisms also metabolize Trp to tryptamine, which is then converted into IAA [3]. The latter can be conjugated with glycine to yield indole-3-acetyl-glycine (IAA-Gly) [4]. Within the serotonin pathway, Trp is hydroxylated by tryptophan hydroxylase 2 and then decarboxylated by aromatic L-amino acid decarboxylase to form serotonin [5]. Serotonin serves as the precursor for melatonin and 5-hydroxy-indole-3-acetic acid (HIAA). About 95% of the ingested Trp enters the kynurenine pathway and is metabolized into kynurenine (KYN), kynurenic acid (KA), anthranilic acid (AA), 3-hydroxykynurenine (HK), 3-hydroxyanthranilic acid (HAA), xanthurenic acid (XA), and quinolinic acid (QA). The kynurenine pathway is also linked to nicotinamide metabolism and the formation of nicotin-

amide (NAm) and nicotinic acid (NA) [6]. Most catabolites are biologically active and involved in the pathogenesis of many disease processes [7–12]. Furthermore, the interrelationship between metabolic pathways is of profound pharmacological and physiological importance as changes in one pathway might have secondary effects on the others [1]. New physiological roles and correlations between the different pathways can only be described by the simultaneous detection of all the metabolites. Liquid chromatography (LC) coupled to electrospray ionization (ESI) and tandem mass spectrometry (MS/MS) is a selective and sensitive tool for the trace analysis of multiple compounds in various matrices. Methods have been developed using LC-MS/MS to quantify melatonin [13], serotonin [13–15], HIAA [16, 17], IAA [13, 18–20], and 3-IS [21]. Amirkhani et al. [22] described a method to determine Trp, KYN, and KA in human plasma by capillary LC-MS/MS. LC-MS/MS was also employed to measure both intracellular and extracellular levels of Trp, KYN, HK, and HAA [23]. In 2009, de Jong et al. [24] developed an LC-MS/MS method that enabled the simultaneous extraction, concentration, separation, and mass selective detection of Trp, KYN, and HK in plasma. The most comprehensive method to date was introduced by Midttun et al. [25], who employed LC-MS/MS to quantify plasma levels of Trp, KYN, HK, KA, AA, XA, and HAA.

However, none of the methods mentioned above covers comprehensively all branches of tryptophan metabolism. Here, we introduce an LC-ESI-MS/MS method for the quantification of Trp and 18 key metabolites within the serotonin, kynurenine, indole-3-pyruvate/tryptamine, and indole pathways, respectively. The method works without prior enrichment or derivatization and uses stable isotope-labeled internal standards for quantification. The method was validated for the analysis of human serum, urine, and cell culture supernatants and was applied to cell culture supernatants from monocytes and dendritic cells with or without IFN-γ treatment.

## Experimental section

### Chemicals and materials

Unlabeled Trp, KYN, KA, AA, HK, HAA, XA, QA, NA, NAm, tryptamine, ILA, IPA, IAA, IAA-Gly, HIAA, serotonin hydrochloride, melatonin, 3-IS potassium salt (3-IS), isatin, $^{2}H_5$-Trp, and $^{2}H_2$-IAA were purchased from Sigma-Aldrich. $^{2}H_4$-AA, $^{2}H_4$-KYN, and $^{2}H_2$-HAA were from Buchem (Apeldoorn, the Netherlands). $^{2}H_4$-tryptamine, $^{2}H_4$-melatonin, $^{2}H_4$–serotonin creatinine sulfate complex, $^{2}H_5$-HIAA, $^{2}H_4$-NA, $^{2}H_4$-NAm, and $^{2}H_5$-KA were from C/D/N Isotopes (Pointe-Claire, Canada). $^{2}H_3$-HK was kindly supplied by I.P. Kema (Department of Laboratory Medicine, University Hospital Groningen, the Netherlands). $^{2}H_3$-QA was kindly supplied by Sanford Markey (Laboratory of Neurotoxicology, National Institutes of Health, Bethesda, MD, USA). Fully $^{13}$C-labeled yeast extracts containing $^{13}C_{10}$-KYN, $^{13}C_7$-HAA, $^{13}C_{11}$-Trp, $^{13}C_{10}$-XA, $^{13}C_{10}$-KA, $^{13}C_7$-QA, $^{13}C_{10}$-HK, and $^{13}C_{10}$-IAA were prepared as described by Wu et al. [26]. $^{2}H_2$-IAA-Gly was prepared in-house according to Bridges et al. [4]. The water used was purified by means of a PURELAB Plus system (ELGA LabWater, Celle, Germany). Solvents for sample preparation and LC-MS analysis were HPLC grade and purchased from Fisher Scientific (Schwerte, Germany) and Merck (Darmstadt, Germany).

### Internal standard preparation and stock solutions

Stock solutions of each deuterated internal standard and $^{13}$C-labeled yeast extract were prepared in water with 0.1% (*v*/*v*) formic acid and stored at −80 °C. The stable isotope-labeled standards were combined in a working solution containing $^{2}H_4$-melatonin and $^{2}H_2$-IAA-Gly (1 μM each); $^{2}H_4$-AA, $^{2}H_4$-tryptamine, and $^{2}H_4$-serotonin (2 μM each); $^{2}H_4$-NA, $^{2}H_4$-NAm, isatin, and $^{2}H_5$-HIAA (10 μM each); as well as 50 mg dry weight yeast extract per milliliter containing $^{13}C_{10}$-KYN, $^{13}C_7$-HAA, $^{13}C_{11}$-Trp, $^{13}C_{10}$-XA, $^{13}C_{10}$-KA, $^{13}C_7$-QA, $^{13}C_{10}$-HK, and $^{13}C_{10}$-IAA. Individual stock solutions of unlabeled analytes were prepared in either water with 0.1% formic acid, water with 0.1 M NaOH, water/methanol, or water/acetonitrile mixtures in concentrations of around 10 mM. Different solvents were used due to varying analyte solubilities. A master mix including Trp at 5 mM and the other compounds at a concentration of 250 μM in water with 0.1% formic acid was generated and serially diluted over a concentration range from 200 μM to 0.5 nM. For calibration, 10 μL of the internal standard solution was transferred into a 0.2-mL micro-insert (VWR, Darmstadt, Germany) in a 1.5-mL glass vial (Fisher Scientific) and then diluted to 100 μL with the respective aqueous calibration standard. The final concentrations of the internal standards spiked into samples and calibration standards were 100 nM ($^{2}H_4$-melatonin and $^{2}H_2$-IAA-Gly), 200 nM ($^{2}H_4$-AA, $^{2}H_4$-tryptamine, $^{2}H_4$-serotonin), 1 μM ($^{2}H_4$-NA, $^{2}H_4$-NAm, isatin, $^{2}H_5$-HIAA), and 5 mg dry weight extract per milliliter ($^{13}C_{10}$-KYN, $^{13}C_7$-HAA, $^{13}C_{11}$-Trp, $^{13}C_{10}$-XA, $^{13}C_{10}$-KA, $^{13}C_7$-QA, $^{13}C_{10}$-HK, $^{13}C_{10}$-IAA), respectively. Stable isotope-labeled analogs were not available for IPA and ILA; thus, $^{2}H_4$-melatonin and $^{13}C_{10}$-IAA were used to calculate the area ratio for ILA and IPA, respectively, because they provided the best recoveries and precision for these analytes.

### Instrumentation

An Agilent 1200 SL HPLC system (Böblingen, Germany) coupled to an Applied Biosystems (Darmstadt, Germany) 4000 QTrap mass spectrometer equipped with a TurboV electrospray ion source and operated in either positive or negative ion mode was used. Analyst v.1.5.1 from Applied Biosystems/MDS SCIEX was used for the acquisition and analysis of data.

A Waters (Eschborn, Germany) Atlantis T3 (2.1×150-mm i.d., 3 μm) reversed-phase column with mobile phases A (0.1% formic acid in water, *v*/*v*) and B (0.1% formic acid in acetonitrile, *v*/*v*) was used. The column was kept at 25 °C. All analytes except for 3-IS were detected in positive ion multiple reaction monitoring (MRM) mode. Chromatographic separation of the analytes detected in positive mode was performed using a linear gradient as follows: 0–10 min linear increase from 0% to 40% B, 10–12 min from 40% to 95% B, 12–12.1 min from 95% to 0% B, and hold at 0% B for 5 min. A separate analysis was performed for 3-IS (detected in negative ion MRM mode) with the following linear gradient: 0–1 min linear increase from 0% to 50% B, hold at 50% B for 5 min, 6–6.1 min from 50% to 0% B, and hold at 0% B for 4 min. The flow rate, at all times, was 0.4 mL/min. The column effluent was delivered to the mass spectrometer with no split. If not otherwise noted, an injection volume of 10 μL was used.

All MS parameters were optimized by direct infusion; the source parameters, by flow injection. The ion source was operated using turbo ion spray with ion spray voltage set at 5,500 or −4,500 V, curtain gas at 10 psig, ion source temperature at 500 °C, ion source gas 1 and 2 at 50 psig, and collision gas at medium. Analytes were detected using multiple reaction monitoring applying the parameters listed in Table 1.

### Preparation of serum, cell culture supernatants, and urine samples

Serum and cell culture supernatants were thawed at room temperature. Sample preparation started within 30 min of thawing the samples. Ten microliters of the internal standard mix was added to 50 μL of serum or cell culture medium. The sample was then diluted to 100 μL with water containing 0.1% formic acid (*v*/*v*), vortexed, followed by the addition of 400 μL of cold methanol, vortexed again, and incubated at −20 °C for 1 h to ensure complete protein precipitation. Samples were centrifuged at 10,000×*g* at 4 °C for 10 min, the supernatant was collected, and centrifuged again to obtain a clear extract. The supernatant was dried using a vacuum evaporator (CombiDancer, Hettich AG, Bäch, Switzerland). The residue was redissolved in 100 μL of 0.1% formic acid in water and centrifuged at 5,000×*g* at 4 °C for 5 min to obtain a clear extract.

For the preparation of urine samples, 10 μL of the internal standard mix was added to 10 μL of urine. The sample was then diluted to 100 μL with 0.1% formic acid in water and centrifuged at 10,000×*g* at 4 °C for 10 min. Serum and urine samples were obtained from healthy volunteers.

## Method validation

### Linear range, LOD, and LOQ

The linear range for each analyte was evaluated using a series of standard solutions with internal standards, and each standard solution was measured five times. The calibration curves were constructed based on peak area ratios of the analytes to internal standards (analyte/IS) versus the corresponding nominal concentration ratio (analyte/IS). Since the exact concentration of the $^{13}$C-labeled analytes in yeast extract is not known, an arbitrary value of 1 was used to set up the calibration curves. Consequently, the alternate use of $^{13}$C- and $^{2}$H-labeled analogs resulted in different slopes of the respective calibration curves.

The linear range is defined by the lower (LLOQ) and the upper limit of quantification (ULOQ). The LLOQ of an analytical procedure is the lowest concentration below which the method could not operate with an acceptable precision and trueness. In accordance with the FDA Guide for Bioanalytical Method Validation, the LLOQ and ULOQ are defined as the lowest and the highest points of the calibration curve with accuracy between 80% and 120% and an imprecision of <20% [27]. The limit of detection (LOD) is the lowest concentration that was detectable in all replicates, but not necessarily quantified [27]. LODs were determined from the linearity data as the lowest concentrations that gave peaks with signal-to-noise (S/N) values equal or higher than 3.

### Recovery and precision

Analyte recovery and precision for the analysis of serum and cell culture supernatants were determined by adding standard working solutions of all candidate analytes at low (40 nM of NA, NAm, HK, serotonin, HAA, tryptamine, XA, KA, HIAA, AA, IAA-Gly, melatonin; 1 μM of QA, KYN, ILA, IAA, IPA, 3-IS; 10 μM of Trp), medium (200 nM of NA, NAm, HK, serotonin, HAA, tryptamine, XA, KA, HIAA, AA, IAA-Gly, melatonin; 2 μM of QA, KYN, ILA, IAA, IPA, 3-IS; 50 μM of Trp), and high concentrations (800 nM of NA, NAm, HK, serotonin, HAA, tryptamine, XA, KA, HIAA, AA, IAA-Gly, melatonin; 4 μM of QA, KYN, ILA, IAA, IPA, 3-IS; 100 μM of

**Table 1** List of chromatographic RT, selected MRM parameters, DP, CE, and CXP for each analyte measured

| Analyte | RT (min) | Q1 mass | Q3 mass | DP | CE | CXP |
|---|---|---|---|---|---|---|
| Period 1 | | | | | | |
| NA | 2.36 | 124.0 | 80.0 | 56 | 31 | 12 |
| [$^2H_4$]NA | 2.34 | 128.0 | 84.0 | 56 | 31 | 12 |
| NAm | 2.75 | 123.0 | 80.0 | 46 | 31 | 4 |
| [$^2H_4$]NAm | 2.72 | 127.0 | 84.0 | 46 | 31 | 4 |
| QA | 3.03 | 168.0 | 149.9 | 41 | 15 | 12 |
| [$^{13}C_7$]QA | 3.01 | 175.0 | 157.0 | 41 | 15 | 12 |
| [$^2H_3$]QA | 3.01 | 171.0 | 153.0 | 41 | 15 | 12 |
| HK | 4.76 | 225.2 | 208.0 | 41 | 13 | 12 |
| [$^{13}C_{10}$]HK | 4.73 | 235.2 | 218.0 | 41 | 13 | 12 |
| [$^2H_3$]HK | 4.74 | 228.2 | 211.0 | 41 | 13 | 12 |
| Serotonin | | 177.2 | 160.1 | 41 | 15 | 12 |
| [$^2H_4$]Serotonin | | 181.1 | 164.0 | 41 | 15 | 12 |
| KYN | 6.26 | 209.1 | 192.0 | 40 | 13 | 14 |
| [$^{13}C_{10}$]KYN | 6.22 | 219.1 | 202.0 | 40 | 13 | 14 |
| [$^2H_4$]KYN | 6.23 | 213.1 | 196.0 | 40 | 13 | 14 |
| Period 2 | | | | | | |
| HAA | 7.25 | 154.2 | 80.0 | 46 | 36 | 14 |
| [$^{13}C_7$]HAA | 7.21 | 161.2 | 85.0 | 46 | 36 | 14 |
| [$^2H_2$]HAA | 7.22 | 156.2 | 82.0 | 46 | 36 | 14 |
| Tryptophan | 7.57 | 205.1 | 118.1 | 39 | 26 | 11 |
| [$^{13}C_{11}$]Tryptophan | 7.53 | 216.1 | 126.1 | 39 | 26 | 11 |
| [$^2H_5$]Tryptophan | 7.54 | 210.2 | 122.0 | 39 | 26 | 11 |
| Tryptamine | 7.79 | 161.0 | 144.0 | 36 | 15 | 12 |
| [$^2H_4$]Tryptamine | 7.77 | 165.0 | 148.0 | 36 | 15 | 12 |
| XA | 8.12 | 206.2 | 160.0 | 56 | 27 | 10 |
| [$^{13}C_{10}$]XA | 8.10 | 216.2 | 169.0 | 56 | 27 | 10 |
| KA | 8.56 | 190.2 | 144.0 | 51 | 30 | 10 |
| [$^{13}C_{10}$]KA | 8.53 | 200.2 | 153.0 | 51 | 30 | 10 |
| [$^2H_5$]KA | 8.53 | 195.2 | 149 | 51 | 30 | 10 |
| HIAA | 9.01 | 192.2 | 146.0 | 31 | 21 | 10 |
| [$^2H_5$]HIAA | 9.00 | 197.2 | 151.0 | 31 | 21 | 10 |
| Period 3 | | | | | | |
| AA | 10.28 | 138.2 | 120.0 | 36 | 15 | 8 |
| [$^2H_4$]AA | 10.26 | 142.1 | 124.0 | 36 | 15 | 8 |
| IAA-Gly | 10.56 | 233.0 | 130.0 | 41 | 23 | 8 |
| [$^2H_2$]IAA-Gly | 10.54 | 235.0 | 132.0 | 41 | 23 | 8 |
| ILA | 11.19 | 206.2 | 130.0 | 36 | 39 | 8 |
| Melatonin | 11.66 | 233.1 | 174.0 | 56 | 21 | 14 |
| [$^2H_4$]Melatonin | 11.62 | 237.1 | 178.0 | 56 | 21 | 14 |
| IAA | 12.37 | 176.2 | 130.0 | 56 | 25 | 8 |
| [$^{13}C_{10}$]IAA | 12.36 | 186.2 | 139.0 | 56 | 25 | 8 |
| [$^2H_2$]IAA | 12.35 | 178.2 | 132.0 | 56 | 25 | 8 |
| IPA | 13.44 | 190.2 | 130.1 | 51 | 22 | 8 |
| Negative ion mode | | | | | | |
| Isatin | 4.86 | 145.9 | 118.0 | −60 | −30 | −11 |
| 3-IS | 5.47 | 212.0 | 80.0 | −45 | −16 | −21 |

*RT* retention time, *DP* declustering potential, *CE* collision energy, *CXP* cell exit potential

Trp). Further sample workup proceeded as described above. These spike-in experiments were performed in triplicate for four different serum samples. For cell culture supernatants, a pooled sample was prepared by combining 100 μL each from 20 different samples. The spike-in experiments were performed in triplicate using this pooled sample.

Analyte concentrations in the spiked samples were determined using the calibration curves. Then, the endogenous concentration, determined from the analysis of the unspiked sample, was subtracted to obtain the spiked concentration. Finally, a linear least square regression between the added and the measured concentrations was performed. The slope of the line is a measure for the analyte recovery across the three spike levels. Recovery experiments were not carried out for urine because no sample preparation except a dilution was performed. However, matrix effects were evaluated as described below.

### Matrix effects

Matrix effects in urine were determined using the internal standard mixture described above, which was added at three different concentration levels. We spiked five different urine specimens at low (half the concentration of the internal standard normally used), medium (concentration of internal standard), and high concentration (twice the concentrations of the internal standards). The ratio of the chromatographic peak area in urine to the corresponding peak area in aqueous standard solution is defined as the recovery describing the matrix effect in urine. Because stable isotope-labeled internal standards were not available for IPA, ILA, and 3-IS, the non-labeled compounds were spiked at low (100 nM of IPA and 1 μM of ILA and 3-IS), medium (200 nM of IPA, 2 μM of ILA, and 4 μM of 3-IS), and high concentrations (400 nM of IPA, 4 μM of ILA, and 8 μM of 3-IS) to calculate their recovery.

We also investigated the matrix effects in serum by analyzing five different serum samples in triplicate that were either prepared and analyzed as described above to determine endogenous analyte levels or spiked after the extraction step with 200 nM of NA, NAm, HK, serotonin, HAA, tryptamine, XA, KA, HIAA, AA, IAA-Gly, melatonin; 2 μM of QA, KYN, ILA, IAA, IPA, 3-IS; and 50 μM of Trp. The analyte recoveries describing the matrix effects (MF) were calculated from the analyte peak areas as follows [25]:

$$\text{Recovery}_{\text{MF}} = \frac{[\text{Analyte peak area}]\text{spiked} - [\text{Analyte peak area}]\text{endogenous}}{[\text{Analyte peak area}]\text{standard solution}} \times 100\%$$

and from peak area ratios as:

$$\text{Recovery}_{\text{MF}} = \frac{[\text{Analyte peak area/IS peak area}]\text{spiked} - [\text{Analyte peak area/IS peak area}]\text{endogenous}}{[\text{Analyte peak area/IS peak area}]\text{standard solution}} \times 100\%$$

Both in serum and urine, a recovery value of 100% indicates that there is no absolute matrix effect. There is signal enhancement if the value is >100% and signal suppression if the value is below 100%.

### Comparison of $^{13}C$ and deuterated internal standard

In our initial method validation experiments, we used a $^{13}C$-labeled yeast extract as the internal standard containing $^{13}C_{10}$-KYN, $^{13}C_7$-HAA, $^{13}C_{11}$-Trp, $^{13}C_{10}$-XA, $^{13}C_{10}$-KA, $^{13}C_7$-QA, $^{13}C_{10}$-HK, and $^{13}C_{10}$-IAA. During the course of the experiments, we replaced these $^{13}C$-labeled internal standards ($^{13}C$-IS) with deuterated internal standards (*d*-IS) that were mostly commercially available and can meet long-term needs. In order to compare the two types of internal standard, we measured five different serum and urine samples in triplicate spiked either with $^{13}C$-IS or with *d*-IS. The recovery was determined using the concentration obtained with the $^{13}C$-IS as the reference set at 100%. The recovery is a measure to test whether the same concentration is obtained with different internal standards.

### Isolation and culture of monocytes and dendritic cells

Monocytes were obtained by leukapheresis of healthy donors, followed by density gradient centrifugation over Ficoll/Hypaque and separation by countercurrent centrifugation (J6M-E centrifuge; Beckmann, Munich, Germany) as described previously [28, 29].

Isolated monocytes were cultured for 24 h with or without IFN-γ (500 U/mL, Promocell, Heidelberg, Germany) in RPMI 1640, 2% AB serum (both from PAN-Biotech GmbH, Aidenbach, Germany), L-glutamine (2 mM), and penicillin/streptomycin (50 U/mL each, all from Life Technologies GmbH, Darmstadt, Germany) at 5% $CO_2$ and 37 °C. Immature dendritic cells (iDC) were generated by culturing monocytes for 7 days in RPMI 1640, 10% fetal calf serum (both from PAN-Biotech) supplemented with antibiotics, L-glutamine,

IL-4 (500 U/mL, Promocell), and GM-CSF (500 U/mL, Leukine/Sargramostim; Immunex, Seattle, WA, USA). Mature DC (mDC) were obtained by adding IL-6 (1,000 U/mL), TNFα (10 ng/mL), IL-1β (10 ng/mL), and $PGE_2$ (1 μg/mL; all cytokines from Promocell) to day 5 iDC for another 2 days. Finally, iDC and mDC were stimulated on day 7 in the presence or absence of 500 IU/ml IFN-γ for 24 h.

### Western blotting

The expression of indoleamine 2,3-dioxygenase (IDO) in monocytes, IDC, and mDC in the presence or absence of IFN-γ was examined by Western blot applying anti-human IDO antibody (diluted 1:1,000; clone ID 177, Alexis Biochemicals, San Diego, CA, USA) to cell lysates separated on 10% SDS gels, blotting to PVDF membranes (Milipore, Billerica, MA, USA), and visualization by ECL (Amersham, GE Healthcare, Piscataway, NJ, USA). Detection of β-actin with an antibody from Sigma-Aldrich (St. Louis, MO, USA) that had been diluted 1:1,000 served as loading control.

### Statistical analysis

Unpaired two-tailed *t* test was used to analyze significant differences between each cell type with or without IFN-γ treatment.

## Results and discussion

### Chromatography and mass spectrometry

The mobile phase composition and the gradient were optimized in order to obtain a good analyte separation. Figure 2 shows a representative chromatogram of a standard mixture of Trp and 17 of its metabolites that could be detected in positive mode. The chromatographic run was divided into three scan periods to minimize the number of transitions monitored in parallel, resulting in 10–14 transitions per period. As shown in Fig. 2, all analytes are baseline separated under the optimized conditions. The corresponding retention times are listed in Table 1. The retention times are consistent from run to run, but with contaminant buildup or general column deterioration, the retention times may drift. The retention times of all compounds were checked for 100 samples that were run over a period of 1 week, and the relative standard deviations were below 5.1% for all analytes.

Using electrospray ionization in positive mode, all analytes showed a strong signal for the quasi-molecular ion $[M+H]^+$, and we selected the transition to the most abundant product ion for all analytes to set up the MRM mode, with the exception of Trp for which the third most abundant fragment ion was used as the product ion in order

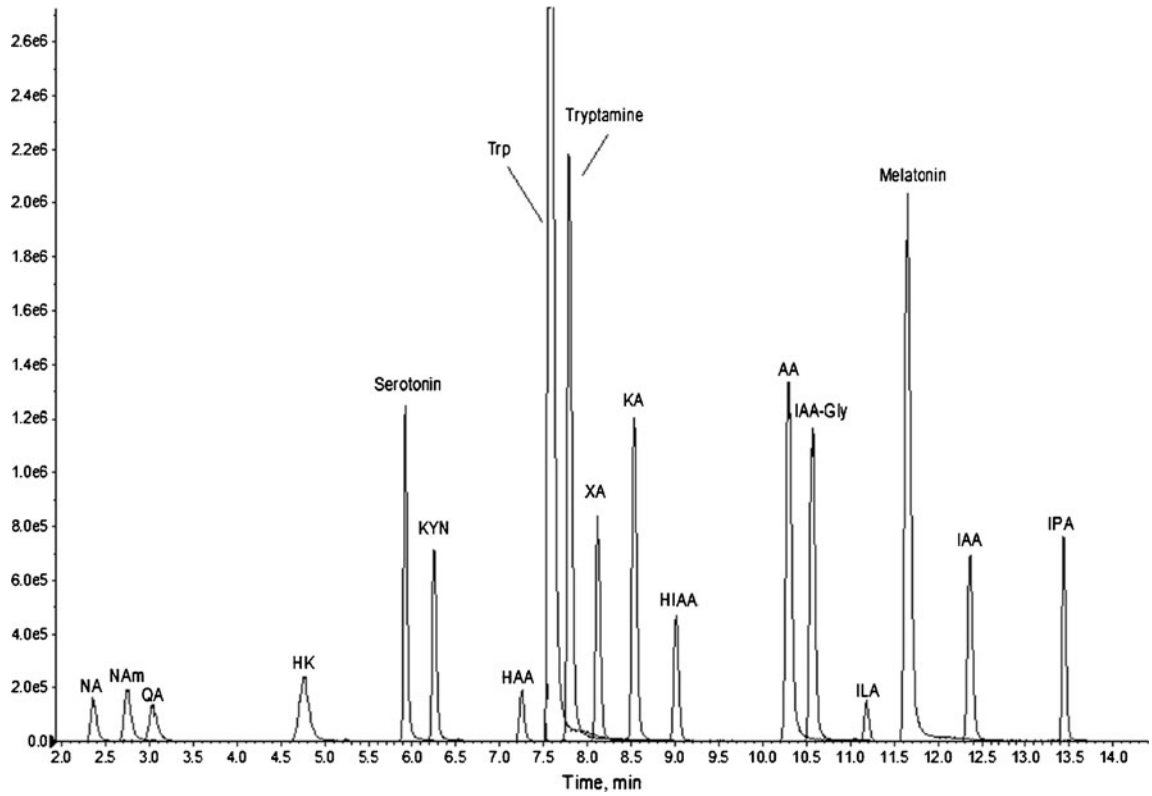


**Fig. 2** Typical LC-MS/MS chromatogram of a standard sample

to avoid detector saturation. The MRM parameters for all analytes are shown in Table 1. In order to minimize the number of transitions monitored in parallel, the chromatographic run was divided into three periods containing between 10 and 14 transitions each (see Table 1). 3-IS and its internal standard isatin were analyzed in a separate LC-MS/MS run using electrospray ionization in negative mode and selecting the quasi-molecular ion and the most abundant fragment ion to set up the MRM transition (see Table 1).

## Calibration

For quantitative analysis, calibration curves were generated for all analytes using $1/X$ weighting. The calibration parameters are summarized in Table 2. The LODs, defined as the concentration producing a peak with an S/N≥3:1, ranged between 0.1 and 3 nM for most compounds, except Trp and QA which had an LOD of 10 and 50 nM, respectively. LLOQs ranged between 0.5 and 5 nM for most metabolites, except for Trp and QA with an LLOQ of 50 and 100 nM, respectively. Most of the LLOQ values are comparable to or lower than those of published LC-MS/MS assays. Cao et al. [13] reported an LLOQ of 0.02 ng/mL (0.1 nM) for melatonin, which is lower than the value reported here. For all other tryptophan metabolites reported in the literature, the LLOQs reported here were lower, including serotonin (5 ng/mL or 28 nM [13], 5 nM [15]); IAA (0.7 ng/mL or 4 nM [13], 5 μg/mL or 29 μM [20]); HIAA (130 nM [17]); KYN (11.2 nM [22], 20 nM [23], 50 nM [24]); KA (11.5 nM [22]); HK (20 nM [23], 23 nM [24]); and HAA (100 nM [23]).

The ULOQ ranged from 1 to 20 μM for the majority of analytes and up to 200 μM for Trp. For 3-IS analyzed by ESI in negative mode, the linear range was from 5.0 nM to 40 μM. The $R^2$ value of the regression analysis over the linear range exceeded 0.99 for all analytes.

**Table 2** Calibration parameters

| Analyte | LOD (nM) | Linear range (nM) | Slope | Intercept | $R^2$ |
|---|---|---|---|---|---|
| NA | 1.0 | 5.0–10,000 | 0.92 | 0.0066 | 0.9991 |
| NAM | 0.4 | 1.0–10,000 | 1.24 | 0.0261 | 0.9989 |
| QA[a] | 50.0 | 100–20,000 | 4.89 | 0.0294 | 0.9995 |
| QA[b] | 50.0 | 100–20,000 | 1.05 | −0.0010 | 0.9999 |
| HK[a] | 1.0 | 2.0–10,000 | 3.56 | 0.0037 | 0.9989 |
| HK[b] | 1.0 | 2.0–10,000 | 39.90 | 0.0078 | 0.9986 |
| Serotonin | 0.6 | 1.0–4,000 | 0.72 | 0.0079 | 0.9985 |
| KYN[a] | 0.4 | 1.0–7,500 | 42.50 | 0.2590 | 0.9972 |
| KYN[b] | 0.4 | 1.0–7,500 | 0.66 | 0.0052 | 0.9940 |
| HAA[a] | 3.0 | 5.0–10,000 | 8.63 | 0.0038 | 0.9992 |
| HAA[b] | 3.0 | 5.0–10,000 | 0.88 | 0.0127 | 0.9996 |
| Tryptophan[a] | 10.0 | 50–200,000 | 1.12 | 0.1290 | 0.9976 |
| Tryptophan[b] | 10.0 | 50–200,000 | 1.66 | 0.0062 | 0.9957 |
| Tryptamine | 0.2 | 0.5–1,000 | 1.15 | 0.0122 | 0.9996 |
| XA[a] | 0.3 | 1.0–5,000 | 32.00 | 0.0431 | 0.9985 |
| XA[b] | 0.3 | 1.0–5,000 | 1.37 | 0.0021 | 0.9984 |
| KA[a] | 0.3 | 1.0–5,000 | 348.00 | 0.5690 | 0.9972 |
| KA[b] | 0.3 | 1.0–5,000 | 0.96 | 0.0039 | 0.9991 |
| HIAA | 2.0 | 5.0–10,000 | 3.84 | 0.0796 | 0.9971 |
| AA | 0.4 | 1.0–1,000 | 0.90 | 0.0186 | 0.9992 |
| IAA-Gly | 0.2 | 0.5–1,000 | 0.98 | 0.0163 | 0.9992 |
| ILA | 1.0 | 5.0–10,000 | 0.42 | −0.0015 | 0.9980 |
| Melatonin | 0.1 | 0.5–1,000 | 0.77 | 0.0149 | 0.9993 |
| IAA[a] | 0.3 | 1.0–7,500 | 97.70 | 6.0200 | 0.9995 |
| IAA[b] | 0.3 | 1.0–7,500 | 1.00 | 0.0020 | 0.9979 |
| IPA[a] | 0.6 | 1.0–7,500 | 82.60 | 0.0847 | 0.9992 |
| IPA[b] | 0.6 | 1.0–7,500 | 0.90 | 0.0006 | 0.9987 |
| 3-IS | 1.0 | 5.0–40,000 | 5.72 | 0.0005 | 0.9991 |

[a]Used $^{13}$C-labeled internal standard

[b]Used $^{2}$H-labeled internal standard

## Spiking experiment

Spike-in experiments using three different spike levels were performed for serum and cell culture supernatants to determine analyte yields from the sample preparation and analysis of the different biological matrices. Each spike level was prepared in triplicate. The average relative standard deviations (RSDs) for serum were below 16% for QA, NAm, KYN, AA, ILA, and IAA-Gly and below 10% for the remaining analytes (see Electronic supplementary material (ESM) Fig. S1a).

A linear regression between the added versus the measured concentration was performed. The slope of the line is a measure of recovery with a slope of 1 indicating 100% recovery. The slopes of the individual analytes for the spike-in experiment in serum are shown in Fig. 3a. Slopes were in the range of 0.79–1.23, indicating good recoveries for all analytes. Standard errors (SEs) were below 0.08 for all analytes.

Stable isotope-labeled internal standard were not available for IPA and ILA. Analyte recovery and RSDs were calculated using several internal standards eluting close to these two analytes. The internal standards that provided the highest recovery (slopes of 0.98 and 0.94) and reproducibility (SE< 0.07) were d4-melatonin for ILA and $^{13}C_{10}$-IAA for IPA.

The average RSDs for the analysis of spiked cell culture supernatants were between 1.0% and 17.4% (see ESM Fig. S1b). Linear regression analysis was performed as described for the serum spike-in experiment (Fig. 3b). Analyte recoveries from spiked cell culture supernatants were between 0.80 and 1.34 at three different spiking levels, with SEs between 0.004 and 0.09.

## Matrix effects

It is well known that the LC-MS response of an analyte may be influenced by the nature of the co-eluting sample matrix, especially when the matrix is complex. A general concern regarding the reliability of any new LC-MS/MS method is ion suppression or enhancement caused by co-eluting compounds. The use of stable isotope-labeled compounds as internal standards is one of the best approaches to correct for matrix effects and improve method accuracy and precision. Although we used a suite of stable isotope-labeled compounds, we still evaluated ion suppression and enhancement.

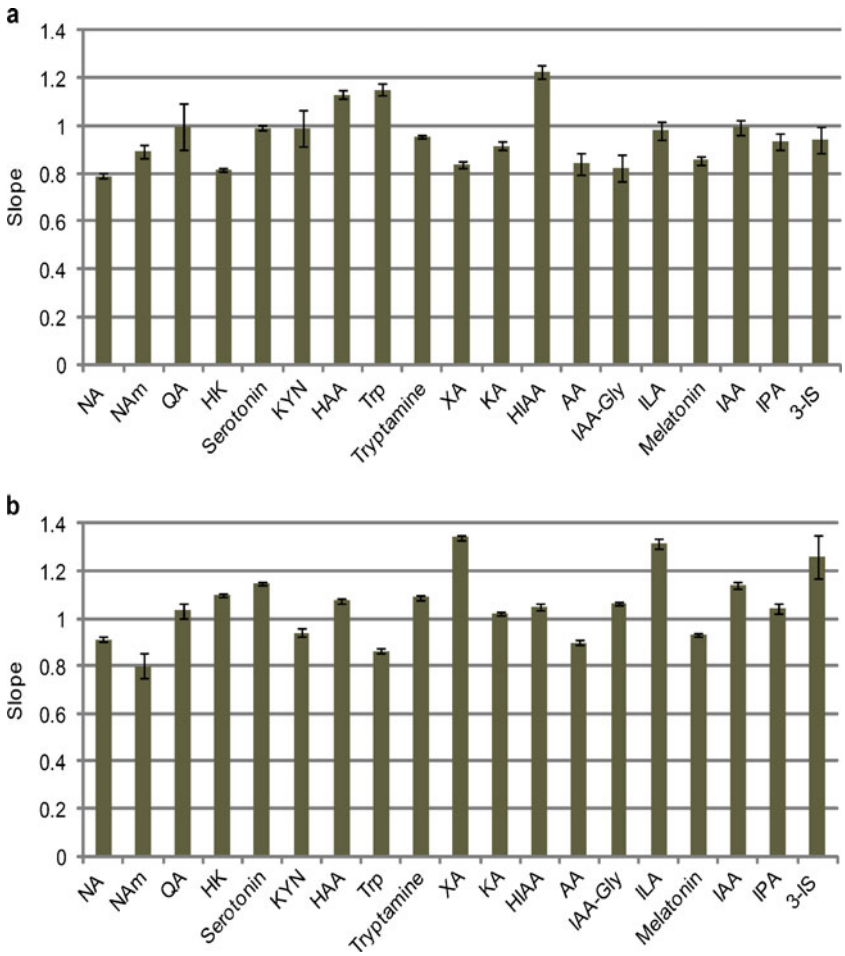


**Fig. 3** Recovery of all analytes at three spiking levels in serum (**a**) ($n$=4) and cell culture supernatant specimens (**b**) ($n$=3), respectively. Recovery is given as the slope of the linear regression between the added and measured concentrations. *Error bars* indicate the standard error

Matrix effects in urine were determined using the internal standard mixture. Five different urine samples were spiked at low, medium, and high concentration. The ratio of the chromatographic peak area in the urine to the corresponding peak area in aqueous standard solution is defined as the recovery describing the matrix effects during the analysis. All analytes with a corresponding stable isotope-labeled internal standards yielded recoveries between 75% and 115% at three different spiking levels (Fig. 4). Despite the lack of a corresponding internal standard, IPA, ILA, and 3-IS showed good recoveries in the range of 99–115%. RSDs were between 1.5% and 13.5%.

We also evaluated the matrix effects in serum because it is the most complex matrix among the three different sample types. To purely evaluate changes in ionization, five different serum extracts were spiked in triplicate with 200 nM of NA, NAm, HK, serotonin, HAA, tryptamine, XA, KA, HIAA, AA, IAA-Gly, melatonin; 2 μM of QA, KYN, ILA, IAA, IPA, 3-IS; and 50 μM of Trp. The analyte peak area after subtraction of the endogenous area count (unspiked extract) was compared to the area integral obtained by analyzing the aqueous metabolite standard. Analyte recoveries in the five different serum samples were found to vary in the range of 60–130% (Table 3). The highest ion suppression was observed for IAA-Gly (recovery of 60%), while ion enhancement was observed for XA (129%). RSDs describing variations between samples ranged from 2.8% to 57.5%, with the highest deviation observed for AA. Dividing the analyte peak area by the area integral of the internal standard corrected for the matrix effects. For most analytes, recoveries were between 87% and 107%, except for AA (71%). RSDs were between 2.2% and 14.0% for all analytes and lower than 10.0% for 16 compounds.

**Table 3** Evaluation of matrix effects in serum samples

| Analyte | Recovery (%) based on analyte/ISTD area ratio | RSD (%) | Recovery (%) based on analyte area | RSD (%) |
|---|---|---|---|---|
| NA | 101.07 | 3.43 | 91.60 | 7.15 |
| NAm | 87.65 | 4.24 | 68.95 | 13.52 |
| QA | 92.21 | 4.23 | 78.55 | 9.34 |
| HK | 95.70 | 2.69 | 106.71 | 4.66 |
| Serotonin | 101.33 | 3.54 | 105.36 | 19.38 |
| KYN | 102.24 | 4.96 | 96.64 | 2.89 |
| HAA | 103.08 | 3.02 | 129.05 | 8.20 |
| Tryptophan | 94.81 | 4.18 | 111.89 | 2.78 |
| Tryptamine | 103.56 | 3.34 | 115.35 | 7.12 |
| XA | 104.57 | 4.27 | 129.40 | 6.29 |
| KA | 103.38 | 7.10 | 116.34 | 6.84 |
| HIAA | 101.98 | 4.95 | 91.54 | 7.58 |
| AA | 71.10 | 14.01 | 74.22 | 57.50 |
| IAA-Gly | 92.59 | 7.98 | 59.95 | 49.72 |
| ILA | 107.24 | 11.65 | 85.38 | 35.75 |
| Melatonin | 100.79 | 2.24 | 78.96 | 43.12 |
| IAA | 92.40 | 8.46 | 94.23 | 18.50 |
| IPA | 91.67 | 11.19 | 92.66 | 13.85 |
| 3-IS | 90.43 | 9.14 | 64.22 | 16.77 |

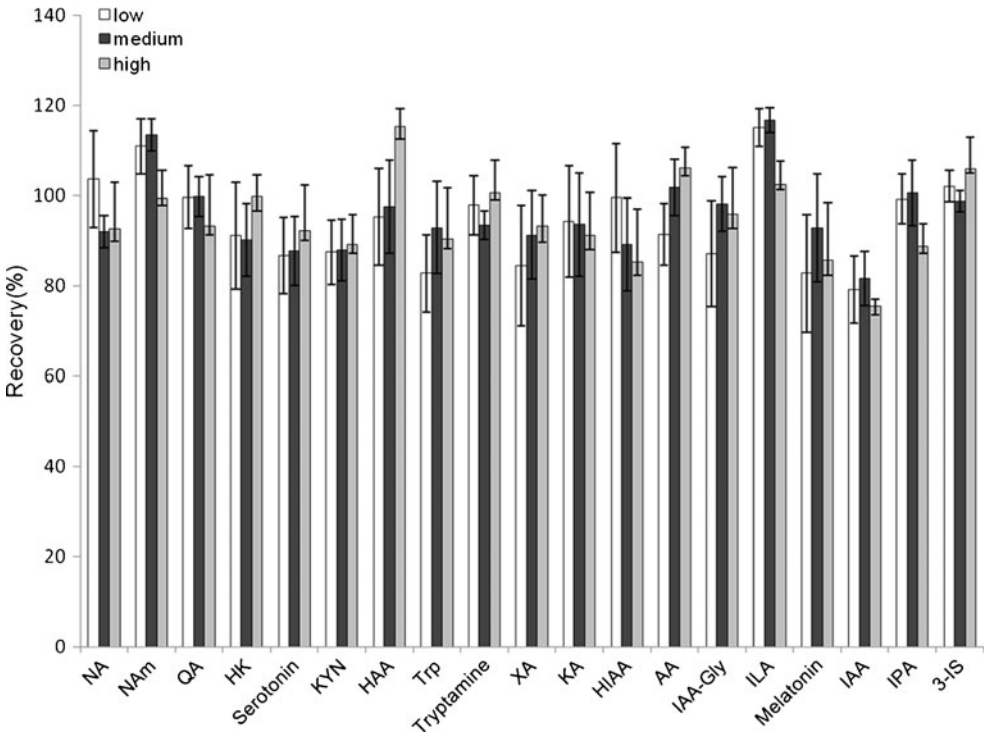


**Fig. 4** Recoveries describing the matrix effects in urine samples. Five different urine samples were spiked at three different concentrations. The ratio of the chromatographic peak area in the urine to the corresponding peak area in aqueous standard solution is defined as the recovery

### Comparison of $^{13}C$ and deuterated internal standards

All the experiments discussed above were performed using $^{13}C$-labeled internal standards. However, during the course of our experiments, we replaced the $^{13}C$-labeled labeled standards from the yeast extract by deuterium-labeled analogs. Calibration parameters obtained with *d*-IS are shown in Table 2. The LODs, LLOQs, ULOQs, and $R^2$ values match the parameters obtained with $^{13}C$-IS. In order to further compare the two types of internal standard, we measured five different serum and urine samples in triplicate spiked with *d*-IS and compared the results with data previously obtained using $^{13}C$-IS. The average RSDs and recoveries over all sample replicates were calculated for all analytes with both *d*-IS and $^{13}C$-IS, with the exception of XA for which a deuterated internal standard was not available. Therefore, XA concentrations were determined using $^{2}H_5$-KA as the reference (Table 4). The data obtained with the $^{13}C$-IS were used as the reference (set 100%) to determine recoveries. Using *d*-IS, the RSDs for all eight analytes in urine and serum were between 2.6% and 7.7% and between 2.9% and 9.7%, respectively. The recoveries using *d*-IS varied from 83% to 100% in urine and from 79% to 112% in serum, demonstrating good correspondence to the data obtained with $^{13}C$-IS. In conclusion, *d*-IS are not only an attractive alternative to $^{13}C$-IS but also carry the advantage of being for the most part available in sufficient amounts from commercial sources.

### Application

To demonstrate the applicability of the method to biomedical specimens, we measured the biological response of monocytes and dendritic cells to stimulation with IFN-γ which is known to induce IDO [30, 31]. The activation of the kynurenine pathway plays an important role in the modulation of the immune system, and in particular, the induction of IDO has been shown to help create a tolerogenic milieu by both the direct suppression of T cells and the enhancement of local Treg-mediated immunosuppression [32].

Monocytes were obtained from two different healthy donors and either left untreated or stimulated with IFN-γ for 24 h. In addition, monocytes were differentiated into iDC or mDC and then treated with or without IFN-γ for 24 h. Western blot analysis confirmed the expression of IDO upon treatment with IFN-γ in monocytes and iDC (see ESM Fig. S2). As described previously, mDC express constitutively high levels of IDO, which was not further enhanced by IFN-γ. Next, we analyzed cell culture supernatants from monocytes, iDC, or mDC after 24 h of incubation with or without IFN-γ as described above to determine changes in the abundance of tryptophan metabolites due to IFN-γ induced IDO. Since IDO catalyzes the first step of tryptophan degradation in the kynurenine pathway, we focused only on metabolites in this pathway. The results for the different donors are shown in ESM Table S1. XA was not detected above the LLOQ in cell culture supernatants from monocytes. HK and HAA were not detected above the LLOQ in cell culture supernatants of monocytes from donor B cultured without IFN-γ. Stimulation with IFN-γ resulted in concentrations of 7 and 120 nM for HK and HAA, respectively, but data showed a high variability of 62.3% (HK) and 83.5% (HAA) for the analysis of cell culture supernatant samples from cells cultured in triplicate. High variability was also observed for QA (32.8%) and AA (27.5%) in samples from monocytes treated with IFN-γ, and HK in control mDC (25.8%) and mDC treated with IFN-γ (41.7%). Otherwise, the RSD values for biological replicates were below 25%.

Figure 5a, b shows the concentration ratios (IFN-γ treatment versus untreated cells) of Trp and KYN metabolites in two individual donors. In case metabolite concentrations were below the LLOQ, the value of the LLOQ was taken to calculate ratios (indicated by #). Analyses of supernatants from monocytes and iDC incubated with IFN-γ for 24 h revealed an increased degradation of Trp accompa-

**Table 4** Performance of deuterated internal standards

| | Urine | | Serum | |
|---|---|---|---|---|
| | Mean RSD (%) | Mean recovery (%) | Mean RSD (%) | Mean recovery (%) |
| Trp | 2.57 | 99.89 | 2.85 | 112.22 |
| KYN | 3.45 | 84.99 | 3.93 | 104.68 |
| HK | 7.67 | 94.47 | 8.28 | 109.99 |
| KA | 4.23 | 86.75 | 3.02 | 103.71 |
| HAA | 4.49 | 96.49 | 9.72 | 79.34 |
| XA | 5.28 | 89.90 | 7.19 | 89.27 |
| QA | 4.70 | 83.24 | 7.25 | 93.57 |
| IAA | 2.67 | 96.92 | 3.13 | 90.73 |

Mean RSD and recoveries were calculated across five urine and serum specimens, respectively, analyzed in triplicate. The data obtained with the $^{13}C$-IS were used as the reference (set 100%) to determine recoveries

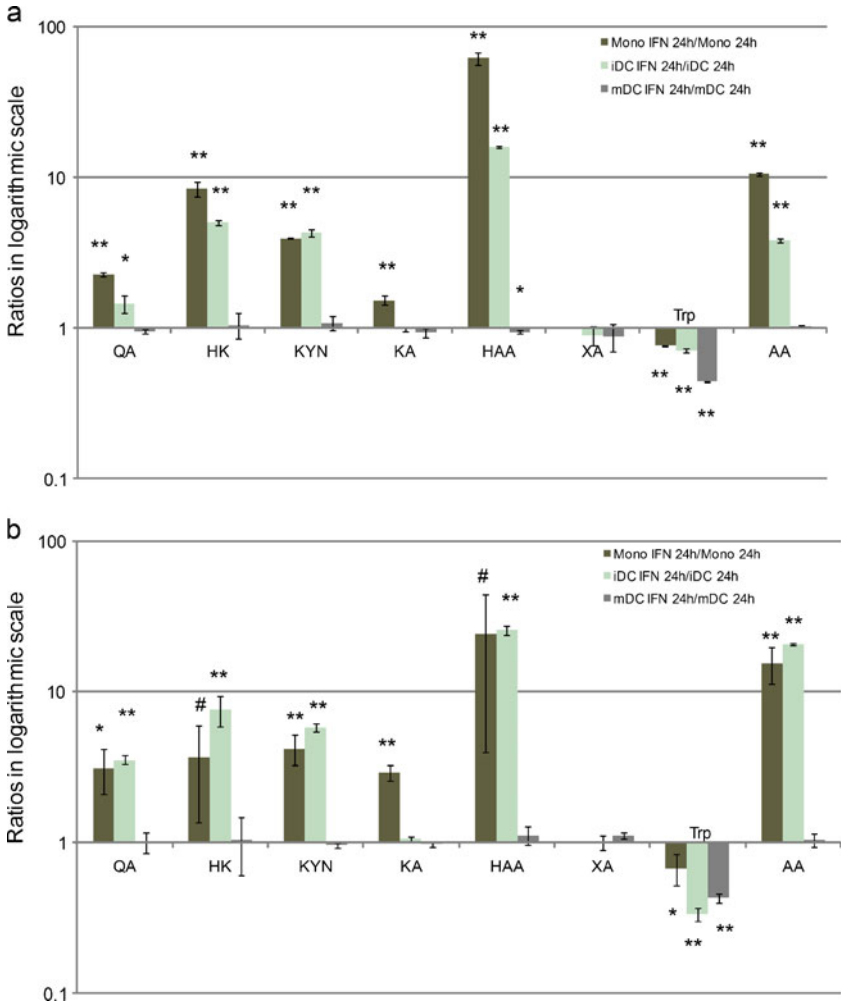


**Fig. 5** **a**, **b** Concentration ratios (with IFN-γ/without IFN-γ) of tryptophan and kynurenine metabolites in cell culture supernatants of monocytes, iDC, and mDC from two different donors (A and B). Cells from each donor were cultivated in triplicate. Significant up- or down-regulation of metabolite concentrations compared with control samples are indicated by $*p<0.05$ and $**p<0.01$. LLOQ values were used to calculate ratios if the metabolite concentration was below LLOQ (indicated by a *number sign*)

nied by an increased release of kynurenine metabolites into the supernatant. In contrast, kynurenine metabolites remained mostly unchanged in supernatant from mDC after incubation with IFN-γ, except for a slight decrease ($p=0.04$) in HAA concentration (donor A) from 4.88 μM (without IFN-γ) to 4.54 μM (with IFN-γ). However, IDO is already highly expressed in mDC even in the absence of stimulation with IFN-γ (see ESM Fig. S2), possibly explaining the lack of changes in the kynurenine pathway. Interestingly, Trp concentrations decreased by more than 50% in mDC supernatants from both donors upon treatment with IFN-γ.

The highest fold change was observed for HAA, which increased ≥62 and ≥16 times in monocytes and iDC cell culture supernatants (donor A) after treatment with IFN-γ. As already discussed above, HAA was below the LLOQ in monocyte cell culture supernatants from donor B, so we used the LLOQ value to calculate the fold changes. As in donor A, HAA shows the strongest relative increase after interferon stimulation. Furthermore, AA, HK, KYN, and QA significantly increased ($p\leq0.05$) in monocytes and iDC cell culture supernatants after treatment with IFN-γ in both donors (see ESM Table S1). KA significantly increased ($p<0.001$) in cell culture supernatants from monocytes upon stimulation with IFN-γ. XA did not significantly change in any of the samples.

The KYN/Trp ratio, reflecting the activity of the IDO enzyme, was significantly higher in the supernatant from cells stimulated with IFN-γ compared with the controls (see ESM Table S1), which correlated with the induction of IDO (see ESM Fig. S2). As already mentioned above, mDC constitutively express IDO, which is reflected by a significantly higher tryptophan consumption and significantly higher concentrations of KYN, QA, HK, KA, HAA, and AA when comparing control samples to mDC and iDCs.

## Conclusions

An LC-ESI-MS/MS method was developed for the quantitative analysis of tryptophan and 18 key metabolites of the serotonin, kynurenine, indole-3-pyruvate/tryptamine, and indole pathways, respectively. With LODs and LLOQs in the lower nanomolar range, the method is sufficiently

sensitive for the direct analysis of these metabolites in biological matrices such as serum, urine, or cell culture medium. Stable isotope-labeled internal standards were used to ensure quantitative precision and accuracy of target analytes. Deuterated and $^{13}C$-labeled internal standards provided high reproducibility.

A significant up-regulation of the tryptophan metabolism along the kynurenine pathway in monocytes and iDC upon IFN-γ stimulation was shown, demonstrating the biomedical applicability of the method.

**Acknowledgments** This project was funded in part by BayGene, the intramural ReForM program of the Faculty of Medicine at the University of Regensburg, and the DFG (KFO 262, DE 835/2-1). We kindly thank Dr. Sanford Markey (Laboratory of Neurotoxicology, National Institutes of Health, Bethesda, MD, USA) for supplying $^{2}H_3$-QA.

## References

1. Keszthelyi D, Troost FJ, Masclee AAM (2009) Neurogastroenterol Motil 21:1239–1249
2. Niwa T (2010) Nagoya J Med Sci 72:1–11
3. Smith EA, Macfarlane GT (1997) Microb Ecol 33:180–188
4. Bridges JW, Evans ME, Idle JR, Millburn P, Osiyemi FO, Smith RL, Williams RT (1974) Xenobiotica 4:645–652
5. Lesurtel M, Soll C, Graf R, Clavien PA (2008) Cell Mol Life Sci 65:940–952
6. Peters JC (1991) Adv Exp Med Biol 294:345–358
7. Suzuki Y, Suda T, Furuhashi K, Suzuki M, Fujie M, Hahimoto D, Nakamura Y, Inui N, Nakamura H, Chida K (2010) Lung Cancer 67:361–365
8. Huttunen R, Syrjanen J, Aittoniemi J, Oja SS, Raitala A, Laine J, Pertovaara M, Vuento R, Huhtala H, Hurme M (2010) Shock 33:149–154
9. Lee SM, Lee YS, Choi JH, Park SG, Choi IW, Joo YD, Lee WS, Lee JN, Choi I, Seo SK (2010) Immunol Lett 132:53–60
10. Gulaj E, Pawlak K, Bien B, Pawlak D (2010) Adv Med Sci 55:204–211
11. De Ravin SS, Zarember KA, Long-Priel D, Chan KC, Fox SD, Gallin JI, Kuhns DB, Malech HL (2010) Blood 116:1755–1760
12. Yan Y, Zhang GX, Gran B, Fallarino F, Yu S, Li H, Cullimore ML, Rostami A, Xu H (2010) J Immunol 185:5953–5961
13. Cao J, Murch SJ, O'Brien R, Saxena PK (2006) J Chromatogr A 1134:333–337
14. Gregersen K, Frøyland L, Berstad A, Araujo P (2008) Talanta 75:466–472
15. Monaghan PJ, Brown HA, Houghton LA, Keevil BG (2009) J Chromatogr B 877:2163–2167
16. Miller AG, Brown H, Degg T, Allen K, Keevil BG (2010) J Chromatogr B 878:695–699
17. de Jong WHA, Graham KS, de Vries EGE, Kema IP (2008) J Chromatogr B 868:28–33
18. Matsuda F, Miyazawa H, Wakasa K, Miyagawa H (2005) Biosci Biotechnol Biochem 69:778–783
19. Durgbanshi A, Arbona V, Pozo O, Miersch O, Sancho JV, Gomez-Cadenas A (2005) J Agric Food Chem 53:8437–8442
20. Hou S, Zhu J, Ding M, Lv G (2008) Talanta 76:798–802
21. Wang G, Korfmacher WA (2009) Rapid Commun Mass Spectrom 23:2061–2069
22. Amirkhani A, Heldin E, Markides KE, Bergquist J (2002) J Chromatogr B 780:381–387
23. Yamada K, Miyazaki T, Shibata T, Hara N, Tsuchiya M (2008) J Chromatogr B 867:57–61
24. de Jong WHA, Smit R, Bakker SJL, de Vries EGE, Kema IP (2009) J Chromatogr B 877:603–609
25. Midttun Ø, Hustad S, Ueland PM (2009) Rapid Commun Mass Spectrom 23:1371–1379
26. Wu L, Mashego MR, van Dam JC, Proell AM, Vinke JL, Ras C, van Winden WA, van Gulik WM, Heijnen JJ (2005) Anal Biochem 336:164–171
27. F.A.D.A. U.S. (2001) Guidance for industry: bioanalytical method validation. Department of Health and Human Services, Center for Drug Evaluation and Research (CDER), Center for Veterinary Medicine (CVM)
28. Andreesen R, Scheibenbogen C, Brugger W, Krause S, Meerpohl HG, Leser HG, Engler H, Löhr GW (1990) Cancer Res 50:7450–7456
29. Stevenson HC, Miller P, Akiyama Y, Favilla T, Beman JA, Herberman R, Stull H, Thurman G, Maluish A, Oldham R (1983) J Immunol Methods 62:353–363
30. Grohmann U, Fallarno F, Puccetti P (2003) Trends Immunol 24:242–248
31. Werner-Felmayer G, Werner ER, Fuchs D, Hausen A, Reibnegger G, Wachter H (1989) Biochim Biophys Acta 1012:140–147
32. Munn DH, Mellor AL (2007) J Clin Invest 117:1147–1154